Int. J. Electrochem. Sci., 13**(2018)** 8428 – 8439, doi: 10.20964/2018.09.55

International Journal of ELECTROCHEMICAL SCIENCE
www.electrochemsci.org

Short Communication

Production of an Activated Carbon from a Banana Stem and its application as electrode materials for Supercapacitors

E.Taer[1,], R. Taslim[2],W.S. Mustika[3], B. Kurniasih[1], Agustino[1], A. Afrianda[1] and Apriwandi[1]*

[1] Department of Physics, University of Riau, 28293 SimpangBaru, Riau, Indonesia
[2] Departement of Industrial Engineering, Islamic State University of Sultan SyarifKasim, 28293 SimpangBaru, Riau, Indonesia.
[3] Department of Physics, Institute of Technology of Bandung, Bandung, West Java, Indonesia
[*]E-mail: erman_taer@yahoo.com

Received: 5 May 2018/ *Accepted:* 2 July 2018 / *Published:* 5 August 2018

The production of activated carbon electrodes from a banana stem for supercapacitor cell applications has been successfully performed. The increase in pore properties was conducted using a KOH chemical activation agent at low concentrations of 0.0, 0.3, 0.5 and 0.7 M, whereas physical activation was performed using CO_2 gas at a temperature of 850 ˚C for 2 h. The activated carbon electrode was fabricated without the addition of adhesive materials. The density, degree of crystallinity, surface morphology, elemental content and surface area of the electrodes were analyzed. The study of electrochemical properties focused on the analysis of the specific capacitance of the supercapacitor cell using cyclic voltammetry. The physical properties of the activated carbon electrodes were correlated to generate the optimum conditions for the specific capacitance of the supercapacitor cells. The optimum specific capacitance obtained at a concentration of 0.5 M KOH reached 170 F/g with a specific surface area of 835.939 m^2/g.

Keywords:banana stem; activated carbon; specific capacitance; supercapacitor

1. INTRODUCTION

Banana (Moses) is a genus of the musaceae family and the order of Zingiberal [1]. In terms of gross production, banana is the world's fourth most important food crop in the world after rice, wheat and corn, and contributing to the economies of many developing countries including Indonesia [2]. The production of bananas in Indonesia reached 6.279.290 tons in 2013 [3]. Ninety percent of banana plants is waste that is not widely used. Unlike banana leaves and fruit, the stems and leaf midrib are usually disposed of and only used on a limited scale such as for planting media [4], fertilizer production [5] and further development as wound medicine. The carbon content in the electrode of

banana stem is very high that reaches 87.86 % [6] so one alternative use of banana plant waste is as a raw material in the preparation of activated carbon electrodes for supercapacitor cell applications. Several studies on the use of banana stems as raw materials in the preparation of supercapacitorelectrodes have been reported [6,7,8]. The preparation process was conducted using a chemical activation agent such as KOH or ZnCl2 at a large concentration of 10-50 percent of the carbon mass. Specific capacitances of supercapacitor electrodes derived from banana stems are104.2 F/g [6], 74 F/g [7], and 156 F/g [8].In the present research, a supercapacitor electrode was fabricated from banana stem waste without any additional adhesive material; it was activated using a KOH activator at a low relative concentration of 0.0 – 0.7 M, followed by a carbonization process at 600 ˚C and physical activation at 850 ˚C for 2 h. The highest specific capacitance reached 170 F/g. The physical properties of the resulting carbon electrode such as the density, surface morphology, degree of crystallinity and surface area were completely evaluated, whereas the specific capacitance of the supercapacitor cell was reviewed based on the variation in the concentration of chemical activation performed. Based on the results from this study it's recommended that the utilization of banana stem waste potentially as a carbon electrode for supercapacitor application.

2. MATERIALS AND METHODS

2.1. Electrodes Preparation

The selected banana stem was banana kapok obtained from smallholder plantations in Riau province, Indonesia. Chemical activation used potassium hydroxide (KOH) agents purchased from Merck KGaA, Germany. The production of activated carbon from banana stems uses a combination of chemical and physical activation. This preparation of the carbon electrode begins by processing banana stems using previously reported methods [9]. Banana stems were pre-carbonized at a low temperature of 250 ˚C for 2.5 hours, followed by a grinding and sieving process, resulting in a green carbon powder with particle sizes of 39-52 μm. The next step, chemical activation, was performed using KOH at various concentrations, i.e., 0.0 M, 0.3 M, 0.5 M, and 0.7 M. All samples were formed into a green carbon monolith by compression pressure, and thus all carbon pellet samples were from integrated carbonization and activation methods, as previously reported [10, 11]. The samples were carbonized at a temperature of 600 °C using a furnace tube in a nitrogen gas environment with a constant flow rate of 1.5 L /min, followed by physical activation using CO_2 gas at a temperature of 850 ˚C and a scan rate of 10 ˚C/min. The carbonization and physical activation processes convert the green monolithic sample into activated carbon (AC), so that each sample is labeled AC-K0, AC-K3, AC-K5 and AC-K7. K-number is concentration of KOH.All AC-Ks were polished and washed to neutral pH to increase the sample purity.

2.2. Physical characteristics

The mass, diameter, thickness, crystallinity, morphology and chemical composition of the activated carbon monolithic samples were measured. The mass, diameter and thickness were recorded to calculate the monolith density of all AC-Ks samples. The crystallinity of the AC-Ks sample was studied X-Ray Diffraction (XRD)using a Philip X-Pert Pro PW 3060/10 instrument with a Cu k-α light source and a wavelength of 1.5418 Å. The diffractogram data was examined in the diffraction angle range of 10-100˚. Interlayer spacing (dhkl) was calculated using the Bragg equation [12], and the microcrystallite dimensions such as the peak height (Lc) and peak width (La) were calculated using the Debye-Scherrer equation [13, 14, 15, 16]. The surface morphology was obtained using scanning electron microscopy (SEM) at 40000-fold magnification, and the chemical composition of the sample was examined using energy dispersive spectroscopy (EDS) with a JEOL JSM-6510 LA instrument.The surface area analysis was analyzed using isothermal adsorption-deasorption Nitrogen (N_2) gas by using Quantachrome NovaWin Version 11.0 instrument.

2.3. Cell fabrication and electrochemical characteristics

The electrochemical property measurements were performed using fabricated supercapacitor cells, i.e., a sandwich type that consists of body cells, current collectors, electrodes, a separator and electrolytes [17]. In this study, AC-Ks were used as supercapacitor electrodes, a 1 M H_2SO_4 solution was selected as the electrolyte, and a duck eggshell membrane was selected as the separator [18]. The body cells and current collectors were made from acrylic and 316 stainless steel tape. Electrochemical measurements were perform using a Physic CV UR Rad-Er 5841 instrument calibrated with a 1280 solartron device. Electrochemical measurement was conducted at a scan rate of 1 mV/s and a potential window of 0 to 500 mV controlled using CVV6 cyclic voltammetry software. Electrochemical characteristics of an AC-Ks-based supercapacitor cell were examined via the specific capacitance calculated using the standard equation [19, 20].

3. RESULTS AND DISCUSSION

3.1. Analysis of mass, diameter, thickness and density

The mass (m), diameter (d), thickness (t) and density (ρ) are reported for the various KOH concentrations in Table 1. AC-K3, AC-K5 and AC-K7 showed a smaller mass and diameter than AC-K0. The difference in mass and electrode diameter due to additional KOH activation can be explained as follows. Chemical activation resulted in KOH impregnation on impurities bonding with carbon materials comparable to KOH concentrations.

Table 1. Mass, diameter, thickness and density of AC-Ks.

Samples	m (g)	d (cm)	t (cm)	ρ (g. cm^{-3})
AC-K0	0.233	1.509	0.168	0.775
AC-K3	0.205	1.471	0.165	0.728
AC-K5	0.176	1.433	0.171	0.639
AC-K7	0.223	1.454	0.161	0.831

The pyrolysis process caused the evaporation of impurity materials that had not been released during chemical activation and are especially present on the surface of the electrode [20]. The release of impurities resulted in a decrease in the mass and diameter. However, AC-K7 showed a mass and a diameter larger than that of AC-K5. The difference in these results is indicated by the shape of the electrode, which in the beginning is already in pellet form, whereas during the carbonization and physical activation process the release of impurities is more active on the surface of the sample. The increase of KOH concentration leaves the activation agent in the inert part of the electrode and it is not released during the pyrolysis process. Meanwhile, the thicknesses show different trends, and AC-K5 has the greatest thickness. Losing mass during the pyrolysis process results in a stronger array of carbon bonds in the electrode samples. Further analysis of the mass, dimensions, diameter and thickness is conducted through the calculated densities. The density is influenced by changes in the mass and dimensions and was smallest for AC-K5. This small density influenced the surface area and capacitive properties of the carbon electrode from a banana stem.

3.2. X-ray Diffraction Analysis

AC-Ks electrode structure data is presented in a X-ray diffractogram shown in Figure 2. All AC-Ks samples exhibit nearly identical diffraction patterns, and the appearance of two broadening peaks in the diffraction data correspond to the carbon amorphous structures [21]. This pattern shows that the atoms are arranged randomly in the sample. The diffraction angle 2θ is identified in the range of 24° for the 002 reflection plane and 44° for the reflection 100 reflection plane. Sharp peaks indicate the presence of small amounts of impurities, such as silica at 2θ = 29˚, which usually appear as biomass burning residues [21]. Potassium hydroxide is at 2θ = 33˚ based on ICDD .cod 01-078-0190 data (ref), and potassium chloride is at 2θ = 40˚ based on ICDD .cod 01-076-3361 data (ref). The sample structure parameters such as the interlayer spacings for the d002 plane and the d100 plane and microcrystallite dimensions such as the peak height [Lc] and peak width [La] were calculated and are listed in Table 2. The d002, d100, Lc and La are obtained in the range of 3.602-3.658 Å, 2.028-2.099 Å, 11.001-14.109 Å and 1.242-2.181 Å, respectively. These data are in the range of carbon material data. The activated carbon from rubber sawdust produces d002, d100, Lc and La in the range of 3.64-3.71 Å, 1.99-2.03 Å, 11.47-22.86 Å and 8.56-21.68 Å, respectively [10]. The d002, d100, Lc and La were obtained in the range of 3.692-3.711 Å, 2.039-2.086 Å, 8.42-10.48 Å and 48.33-52.22 Å, respectively, and have been reported for activated carbon made from palm oil empty fruit branches

[22]. Parameters of crystallite dimensions La and Lc can be further analyzed as Lc/La and Lc/d002 ratios, respectively.

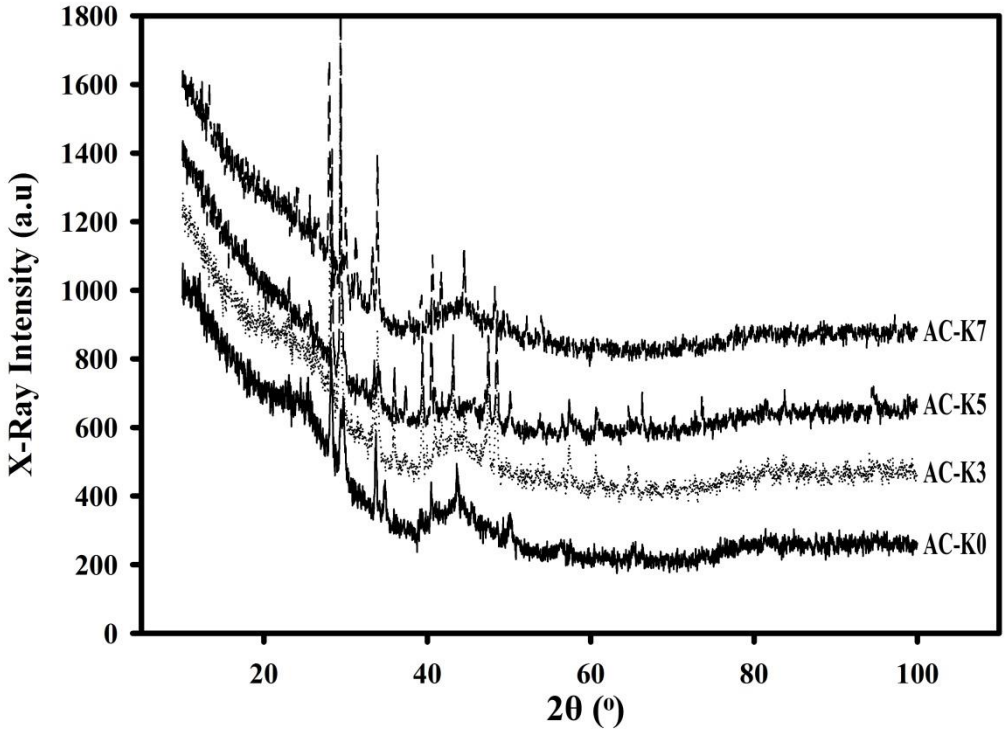

Figure 1. Diffractogram curves of AC-Ks.

The smallest Lc/La and Lc/d002 ratios were obtained at a concentration of 0.5 M KOH. The combination of these two ratios affects the surface area and the capacitive properties of the electrode [23]. The chemical activation on the AC-Ks samples generally increases the d002 and d100 parameters but does not show a trend for increasing KOH concentrations. The KOH activation agent breaks the bonding of impurity materials and carbon atoms through the impregnation reaction [24]. The heating process causes the impregnation of KOH to evaporate to obtain the development of pore structure. As a result, KOH activation changes the lattice arrangement of carbon atoms in the electrode. The increase in KOH concentration in AC-K5 leads to impurity bonding, and more carbon atoms are released compared to AC-K3. Meanwhile, the increase in KOH concentration in AC-K7 produces a bond between KOH and carbon atoms, due to an imperfect washing process. The XRD analysis indicates that the AC-K5 sample has the best pore and capacitive properties, which are shown in the N_2 gas absorption-desorption analysis and the specific capacitance in the next section.

Table 2. Angles of diffraction, interlayer spacing and microcrystallite dimensions of AC-Ks.

Cells	d_{002} (Å)	d_{100} (Å)	L_c (Å)	L_a (Å)	L_c/ L_a	L_c/d_{002}
AC-K0	3.602	2.028	14.109	2.181	6.469	3.917
AC-K3	3.618	2.077	13.274	1.332	9.965	3.669
AC-K5	3.618	2.099	11.001	1.514	7.265	3.041
AC-K7	3.658	2.067	12.116	1.242	9.755	3.312

3.3.Scanning Electron Microscopy

The effect of KOH chemical activation on the surface morphology of activated carbon electrodes from banana stems is reviewed in Figure 2. SEM micrographs show that the samples prepared with the KOH activation agent have more pores than those prepared without KOH. The AC-K0 sample was prepared without chemical activation and contains fiber structures such as an agglomeration of fibers 202-353 nm in size. The AC-K3, AC-K5 and AC-K7 samples show smaller fibers than AC-K0, and they yield a fiber structure in the size range of 95-131, 75-131 and 42-67 nm, respectively. KOH as a chemical activation agent can separated the existing fibers in the banana stem material so that increasing the KOH concentration in the sample decreases the fiber diameter. Chemical activation successfully reduces the fiber size because the activation agent breaks the bonds between the fine fibers. The fine fibers act as bridges between the particles so that the diffusion of ions in the electrode increases. The fiber structure affects the ion diffusion process between carbon particles and increases the capacitive properties of the electrodes.

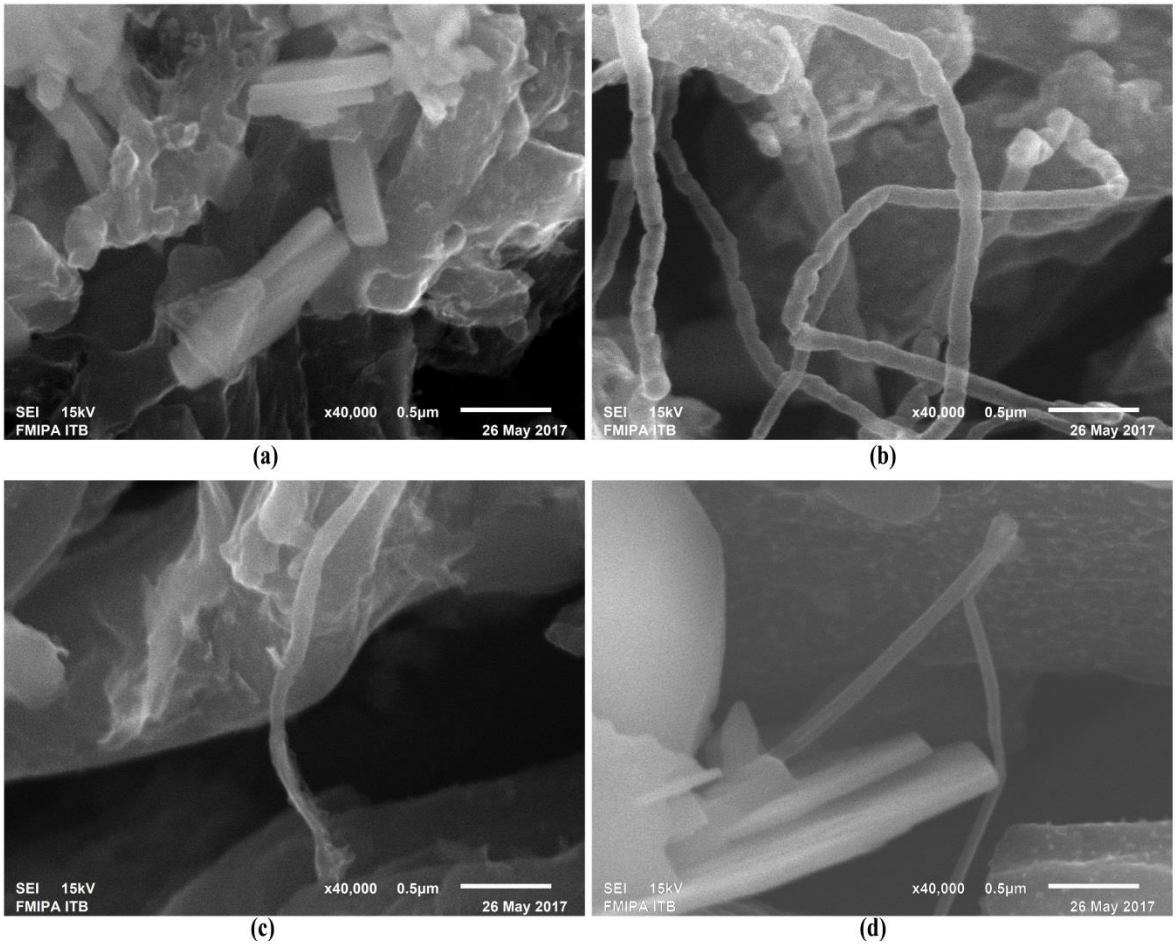

Figure 2. Micrograph SEM of a) AC-K0, b) AC-K3, c) AC-K5, d) AC-K7.

3.4. Energy Dispersive X-ray Analysis

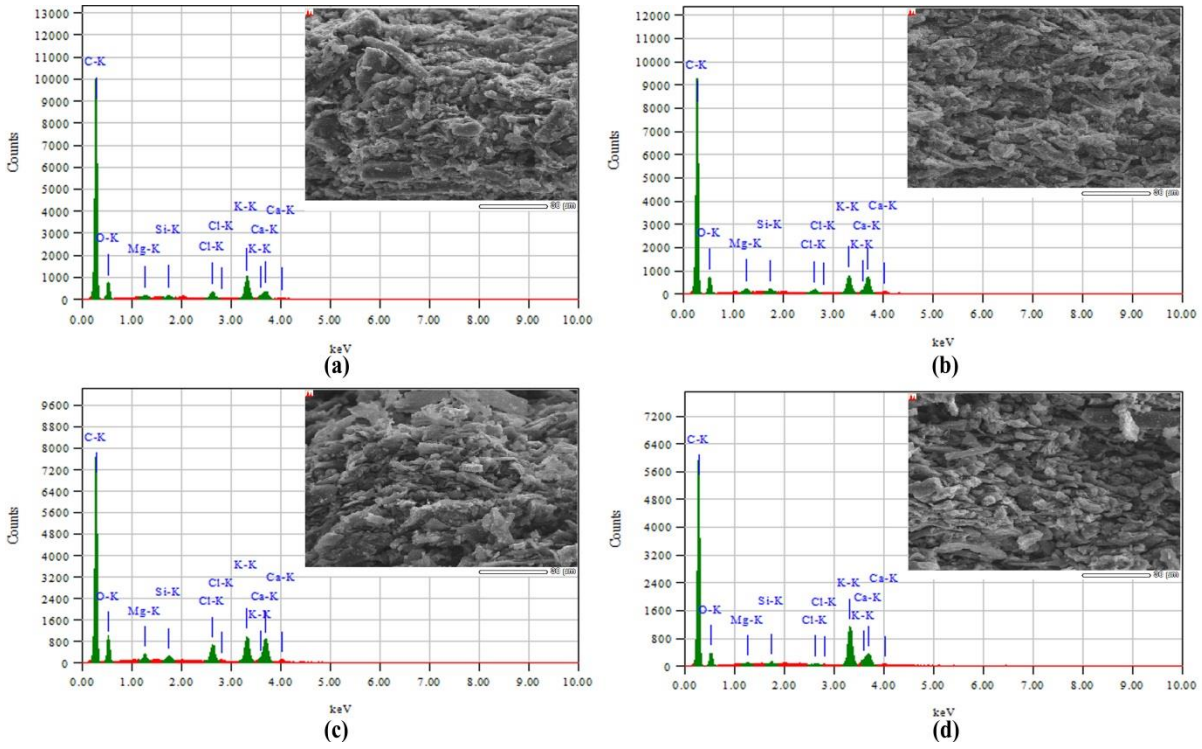

Figure 3. EDS spectra for a) AC-K0; b) AC-K3; b) AC-K5; b) AC-K7.

Table 3. Data EDX for all of AC-Ks

	Atom (%)			
	AC-K0	**AC-K3**	**AC-K5**	**AC-K7**
Carbon	88.76	87.67	84.57	88.15
Oxygen	9.16	9.90	12.03	8.46
Magnesium	0.08	0.16	0.23	0.08
Silica	0.09	0.12	0.14	0.07
Clorin	0.28	0.14	0.65	0.07
Kalium	1.18	1.02	1.19	2.44
Calsium	0.45	1.00	1.19	0.74
Total	100%			

The EDS spectrum of the AC-Ks electrode presents chemical composition data and is shown in the Figure 3. This spectrum shows that the samples are composed of the same elements, namely, carbon, oxygen, magnesium, chlorine, potassium and calcium, and that the carbon content has the highest percentage, 88.76%, 87.67%, 84.57% and 88.15% for AC-K0, AC-K3, AC-K5 and AC-K7, respectively. Chemical activation using KOH affects the quantity of oxygen, potassium and chlorine so that the percentage of carbon changes. The resulting carbon content data are similar to that of other studies on bamboo waste [25] and palm dates [26]. Activated carbon from bamboo waste with steam

activation has a carbon content of 81.18%, and that from palm dates with CO_2 activation has a carbon content of 77.83%. In addition, certain types of impurities such as silica, oxygen, magnesium, chlorine, potassium and calcium are present. These data support the results presented on XRD measurements. The other elements such as magnesium, chlorine, potassium and calcium are the basic ingredients of banana stems. The processes of carbonization and activation at a temperature of 900 °C do not cause these elements to decompose completely. The presence of silica in the sample is due to the influence of the combustion process of the biomass material.

3.5. The analysis of surface area

The isothermal adsorption-desorption nitrogen gas (N_2) analysis of the AC-Ks sample is shown in Figures 4 a) and b). Figure 4 a) shows the relationship between the absorption-desorption volume and N_2 gas relative pressure. The curve shows the form of hysteresis from 0.4 to 1 in relative pressure, P/P_0. The maximum volume of gas absorbed is 306.5976 cm^3/g at a relative pressure of 0.9579 atm. Given the relatively low P/P_0 ratio, the formation of the micro pores of the carbon core further increases the P/P_0 pressure ratio, indicating the formation of larger pores in the carbon material [27]. The adsorption-desorption pattern generated from AC-K5 is of type IV based on the IUPAC classification, indicating a mesoporous range dominant presence in the sample [28]. The average pore produced from the curve is mesoporous with a diameter ranging from 2 nm to 50 nm. The correlation between pore absorption-desorption volume and the pore size distribution of the AC-K5 sample is shown in Figure 4 b). The surface area was analyzed using the Brauner-Emmet-Teller (BET) method, and it reached 835.939 m^2/g. The pore size distribution was evaluated using the Barret-Joyner-Halenda (BJH) model, and dominant absorption data were found at a pore size of 36.1108 Å [29]. These data support the conclusion that the pore type produced from the fiber activated carbon sample is in the mesoporous region with a pore surface area of 63.143 m^2/g.

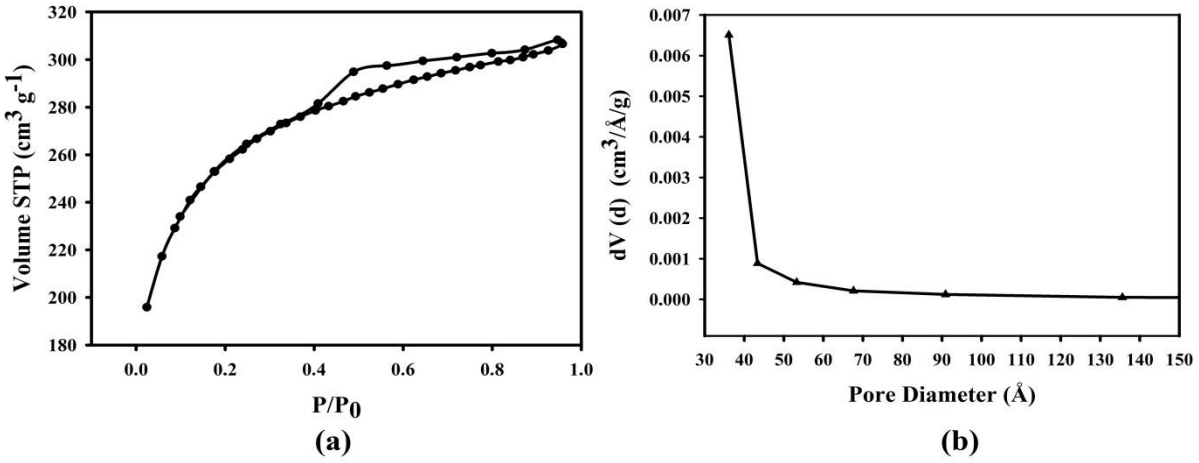

Figure 4. a) Nitrogen adsorption–desorption isotherms; b) Pore size distribution curves for AC-K5.

3.6.Cyclic Voltammetry

Cyclic voltammetry (CV) measurements were reviewed regarding the effect of the KOH activation agent concentration on the electrochemical properties of the AC-Ks samples. AC-Ks electrochemical measurement data are determined from the curve of the plot of the charge-discharge current density versus the potential, which was recorded in a potential window of 0-0.5 V [30], as shown in Figure 5. The overall data show that all the AC-Ks samples prefer a rectangular shape [31], but they differ in the charge-discharge current area. The maximum charge-discharge area was obtained for the AC-K5 sample. The electrochemical properties of AC-Ks supercapacitor cells are further analyzed in terms of specific capacitance values (Csp). Chemical activation using KOH successfully increased the Csp of the AC-Ks samples, i.e., 103 F/g, 139 F/g and 170 F/g for AC-K0, AC-K3 and AC-K5, respectively. The chemical activation produces new pores and increases the surface area, which is proportional to the of concentration of the KOH activation agent. The large surface area provides a large medium for the diffusion of ions into the carbon matrix so that the number of electron-ion pairs increases. These results are consistent with the SEM data, which show that chemical activation succeeded in reducing the fiber to nanometer-sized fine fiber, thus increasing the diffusion of ions between particles. On the other hand, the increase in KOH concentration in the AC-K7 sample reduced Csp to 137 F/g. In conclusion, 0.5 M KOH is the best condition for production of activated carbon for the supercapacitor electrode with the highest specific capacitance, reaching 170 F/g.

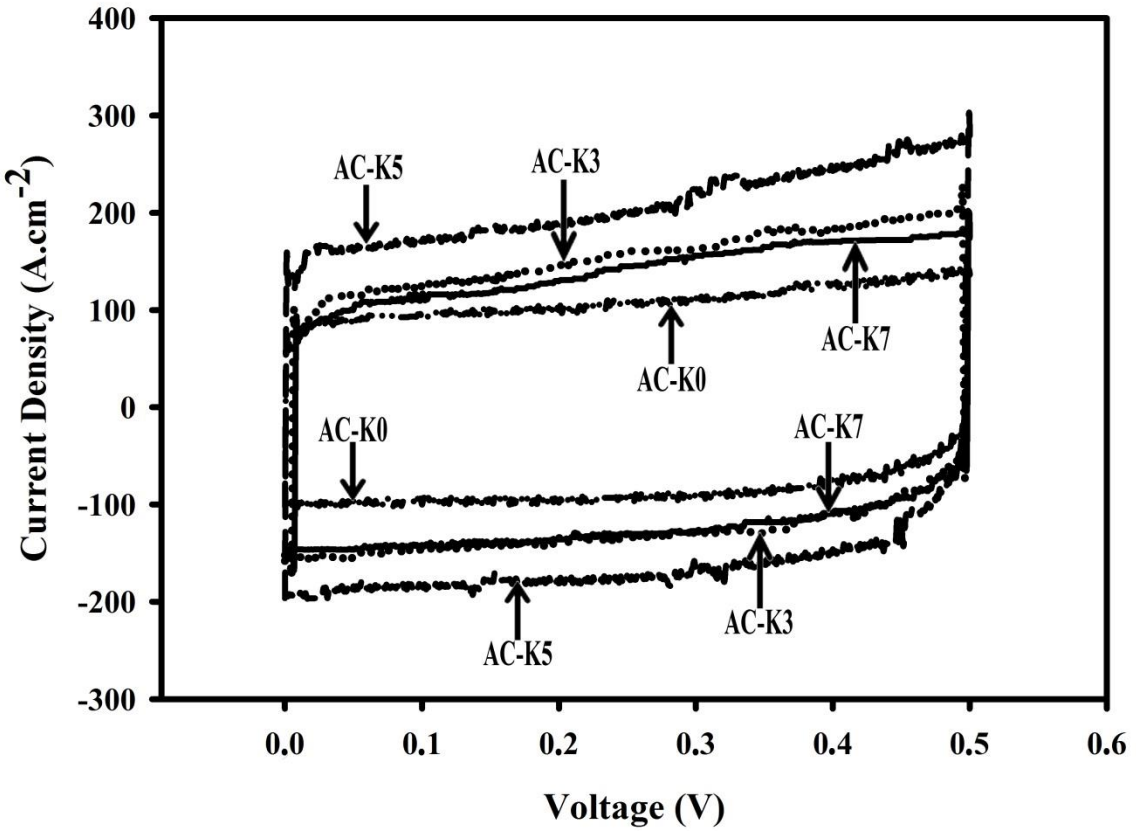

Figure 5. CV curves of all sampels.

The specific capacitance obtained in this study reached 170 F/g, which is higher than104.2 F/g [6], 74 F/g [7], 156 F/g [8] from previous reports and for different biomass can be seen in Table 4. These differences in capacitive properties may be due to the preparation of activated carbon electrodes without additional adhesives material. In our results, an optimum surface area of 835.939 m²/g was obtained, whereas Subramanian et al. reported the surface area of activated carbon from a banana stem as 1097 m^2/g with a specific capacitance reaching 74 F/g [7], comparison of surface area for different biomass shown in Table 4. The surface area of our samples is lower, but it produced a higher specific capacitance. This result is clearly due to the preparation process of the electrodes, in which the addition of adhesive material inhibits or reduces the sizes of existing pores, thereby reducing the supercapacitor capacitive properties. Thus, it is concluded that monolithic activated carbon with a small surface area can produce a higher specific capacitance.

Table 4. Comparison of BET surface area (S_{BET}) and specific capacitance (Csp) of electrodes from different biomass.

Biomassa	**S_{BET} ($m^2.g^{-1}$)**	**Csp ($F.g^{-1}$)**	**References**
Poplar wood	416	234	[32]
Apiaria	895	177	[33]
Coffee shell	842	156	[34]
chitin seafood	759	95	[35]
Patato waste residue	-	255	[36]
Camellia olleifera shell	1935	374	[37]
Sunflower seed shell	2509	311	[38]
Bamboo powder	-	218	[39]
Banana Stem	1097	170	Present study

4. CONCLUSION

The binderless activated carbon electrode from a banana stem exhibits an excellent combination of physical and electrochemical properties. The use of a low concentration of KOH activation agent of 0.0-0.7 M, followed by physical activation at a temperature of 850 ˚C for 2 hours using CO_2 gas, has succeeded in producing an activated carbon electrode without addition of adhesive material. The physical properties of the carbon electrode are strongly related to the specific capacitance of the supercapacitor cell. The density and peak height of the carbon electrode are inversely proportional to the surface area. The lowest density and peak height of the carbon electrode are 0.639 g/cm^3 and 11.001 Å, respectively, and this electrode has the highest specific capacitance of 170 F/g, obtained at a KOH activation concentration of 0.5 M. It can be concluded that the preparation method for activated carbon electrodes from banana stems used herein is a very feasible method for the production of supercapacitor cells.

ACKNOWLEDGEMENTS
The author would like to thank the Riau University through DIPA LPPM with the title "ElektrodaKarbonNanofiberBerbasisBahanAlamUntukPirantiPenyimpanEnergi" with contract

number: 661/UN.19.5.1.3/PP/2018. The author also thanks the SEM FMIPA ITB Laboratory, which has assisted in obtaining the SEM and EDX data.

References

1. I.S. Arvanitoyannis, A. Mavromatis, CriticalReviews inFood Science and Nutrition, 49 (2009) 113.
2. P. Arias, C. Dankers, P. Liu, P. Pilkauskas, The world banana economy: 1985-2002. FAO Commodity studies 1, (2003)FAO, Roma.
3. Badan Pusat Statistik, ProduksiTanaman Pisang Seluruh Provinsi. accessed www.bps.go.id.
4. E. Setianingsih, N. Herlina, L. Setyobudi, *Jurnal Produksi Tanaman,* 04 (2016) 117.
5. A.S. Wulandari, I. Mansur, H. Sugiarti, *Jurnal Silvikultur Tropika,* 03 (2011) 78.
6. E. Taer, Y. Susanti, Awitdrus, Sugianto, R. Taslim, R.N. Setiadi, S. Bahri, Agustino, P. Dewi, B. Kurniasih, *AIP Conf. Proc.,* 1927 (2018) 030016-1.
7. V. Subramanian, C. Luo, A.M. Stephan, K.S Nahm, S. Thomas B. Wei, *J. Phys. Chem. C*., 111 (2007) 7527.
8. K. Chaitra,R.T. Vinny,P.N. Sivaraman, K. Reddy,Venkatesh, N. Nagaraju, N. Kathyayini,C.S. Vivek, *Journal of Energy Chemistry*, 26 (2017) 56.
9. E. Taer, R.Taslim, *AIP Conf. Proc*., 1927 (2018) 020004-1.
10. E. Taer, M. Deraman, I. A. Talib, A. Awitdrus, S.A. Hashmi, *Int. J. Electrochem. Sci*., 6 (2011) 3301.
11. E. Taer, Apriwandi, Yusriwandi, W.S. Mustika, Zulkifli, R. Taslim, Sugianto, B. Kurniasih, Agustino, P. Dewi, *AIP Conf. Proc.,* 1927 (2018) 030036-1.
12. L. Fuhu, C. Weidong, S. Zengmin, W. Yixian, L. Yunfang, L. Hui, *Fuel Process Technol.*, 91 (2010) 17.
13. P.J.M. Carrott, J.M.V. Nabais, M.M.L. R Carrott, J.A. Pajares, *Carbon,* 39 (2001) 1543.
14. B.D. Cullity, Elements of X-Ray Diffraction, Ed. 3, (2001) Amazon Prentice Hall.
15. Awitdrus, M. Deraman, I.A. Talib, R. Omar, M.H. Jumali, E. Taer, M.H. Saman, *Sains Malaysiana,* 39 (2010) 83.
16. J.M.V. Nabais, J.G. Teixeira, I. Almeida, *Bioresour. Technol.,* 102 (2010) 2781.
17. A. González, E. Goikolea, J.A. Barrena, R. Mysyk, *Renewable and Sustainable Energy Reviews*, 58 (2016) 1189.
18. E. Taer, Sugianto, M.A. Sumantre, R. Taslim, Iwantono, D. Dahlan, M. Deraman, *Adv. Materials Research*, 896 (2014) 66.
19. L. Li, E. Liu, J. Li, Y. Yang, H. Shen, Z. Huang, X. Xiang, W. Li*, Journal of Power Sources,*195 (2010) 1516.
20. E. Taer, P. Dewi, Sugianto, R. Syech, R. Taslim, Salomo, Y. Susanti, A. Purnama, Apriwandi, Agustino, R.N. Setiadi, *AIP Conf. Proc.*, 1927 (2018) 030026-1.
21. M. Deraman, R. Omar, S. Zakaria, I.R. Mustapa, M. Talib, *Journal of Material Science*, 37 (2002) 3329.
22. F. Farma, M. Deraman, A. Awitdrus, I.A. Talib, E. Taer, N.H. Basri, J.G. Manjunatha, M.M. Ishak, B.N.M. Dollah, S.A. Hashmi, *Bioresour.Technol.*, 132 (2013) 254.
23. M. Deraman, R. Daik, S. Soltaninejad, N.S.M. Nor, Awitdrus, R. Farma, N. F. Mamat, N.H. Basri, M.A.R. Othman, *Adv. Materials Research,* 1108 (2015) 1.
24. Z. Yue, J. Economy, the textile intitute. (2017) Woodhead Publishing.
25. Y.Z. Zhang, Z.J. Xing, Z.K. Duan, M. Li, Y. Wang, *Applied Surface Science,* 315 (2014) 279.
26. M. Shoaib, H. M. Al-Swaidan, *Biomass and bioenergy,* 73 (2015) 124.
27. W.R. Li, D.H. Chen, Z. Li, Y.F. Shi, Y. Wan, G. Wang, Z.Y. Jiang, D.Y. Zhao, *Carbon*, 45 (2007) 1757.

28. W.S.K. Sing, H.D. Everett, W.A.R. Haul, L. Moscou, A.R. Pierotti, J. Rouquerol, T.Siemieniewska, *Pure & App. Chem.,* 57 (1985) 603.
29. X. Wu, X. Hong, Z. Luo, K.S. Hui, H. Chen, J. Wu, K.N. Hui, L. Li, J. Nan, Q. Zhang, *Electrochem. Acta,* 89 (2013) 400.
30. M. Inagaki, H. Konno, O. Tanaike, *Journal of Power Sources,* 195(2010) 7880.
31. A.M. Abioye, F.N. Ani, *Renewable and Sustainable Energy Reviews,* 52 (2015) 1282.
32. M.C. Liu, L.B. Kong, P. Zhang,Y.C. Luo, L. Kang, *Electrochem. Acta,* 60 (2012) 443.
33. L. Deng, W. Zhong, J. Wang, P. Zhang, H. Fang, L. Yao, X. Liu, X. Ren, Y. Li, *Electrochem. Acta,* 228 (2017) 398.
34. M.R. Jisha, Y.J. Hwang, J.S. Shin, K.S. Nahm, T.P. Kumar, K. Karthikeyan, N. Dhanikaivelu, D. Kalpana, N.G. Renganathan, A.M. Stephan, *Material Chemistry and Physics,*115(2009) 33.
35. B. Duan, X. Gao, X. Yao, Y. Fang, L. Huang, J. Zhou, L. Zhang, *Nano Energy,* 27(2016) 482.
36. M. Ma, Q. Yang, K. Sun, H.Peng, F. Ran, X. Zhao, Z. Lei, 2015,*Bioresour. Technol*., 197(2015) 137.
37. J. Zhang, L. Gong, K. Sun, J. Jiang, X. Zhang,*Journal of Solid StateElectrochemistry*, 16 (2012)2179.
38. X. Li, W. Xing, S.Zhuo, J. Zhou, F. Li, S.-Z.Qiao, G.-Q. Lu,*Bioresour.Technol.,* 102(2011)1118.
39. Y. Zhang, F. Wang, H. Zhu, L. Zhou, X.Zheng, X. Li, Z. Chen, Y. Wang, D. Zhang D. Pan, *Journal Surface Science*, 426(2017)99.

© 2018 The Authors. Published by ESG (www.electrochemsci.org). This article is an open access article distributed under the terms and conditions of the Creative Commons Attribution license (http://creativecommons.org/licenses/by/4.0/).